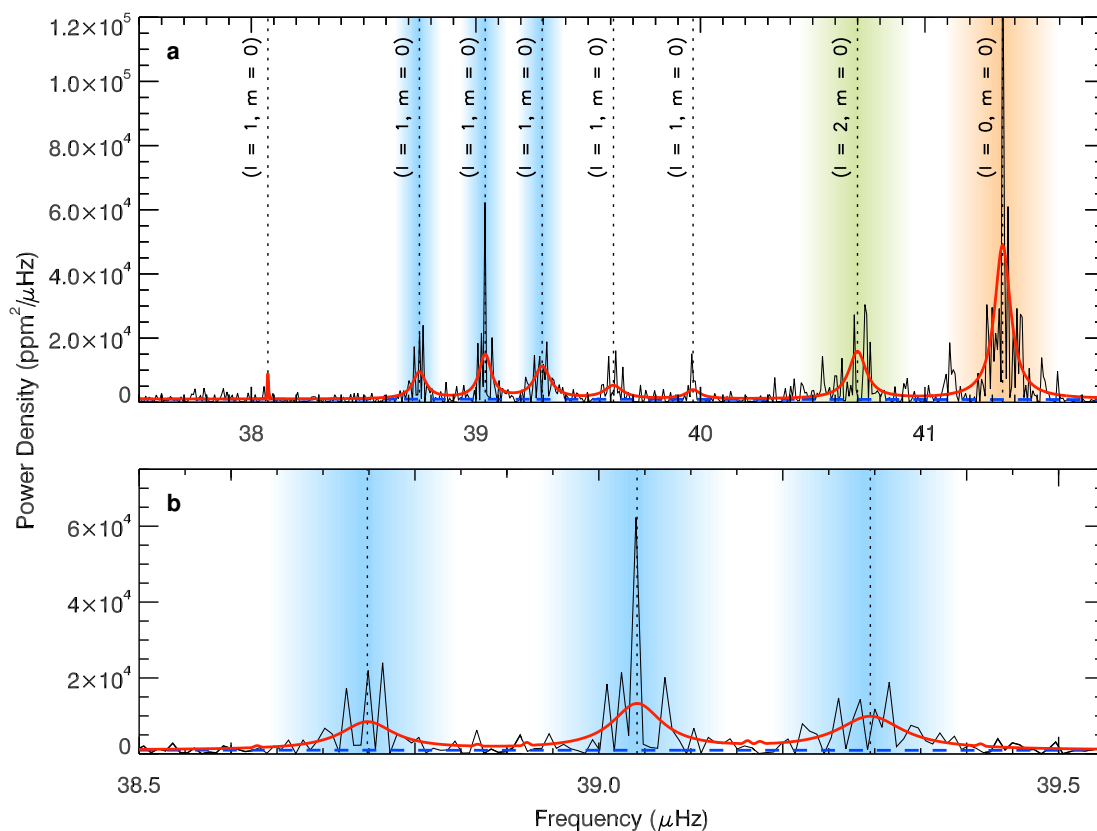




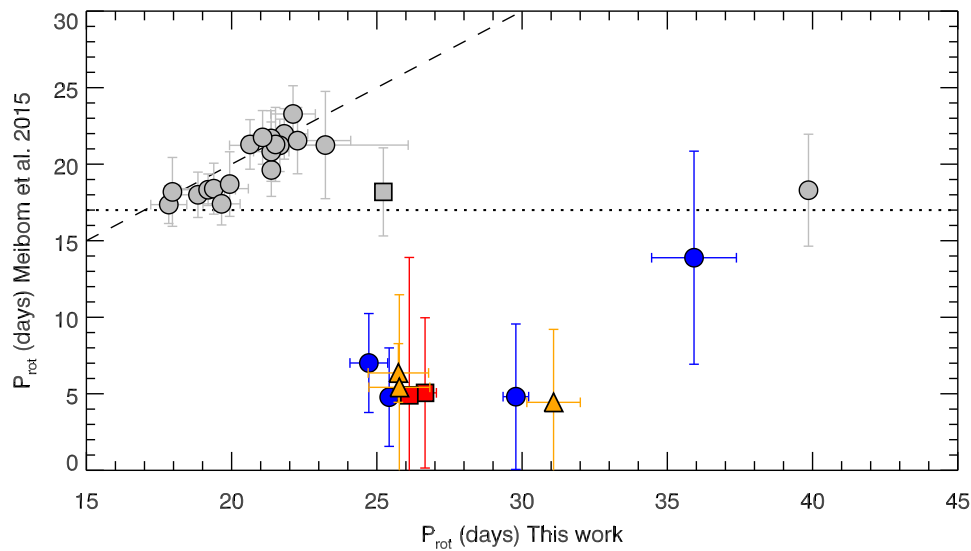
|                                  |  |
|----------------------------------|--|
| <b>Publication Year</b>          | 2017   |
| <b>Acceptance in OA</b>          | 2020-09-04T13:00:48Z   |
| <b>Title</b>                     | Spin alignment of stars in old open clusters   |
| <b>Authors</b>                   | CORSARO, ENRICO MARIA NICOLA, Lee, Yueh-Ning, García, Rafael A., Hennebelle, Patrick, Mathur, Savita, Beck, Paul G., Mathis, Stephane, Stello, Dennis, Bouvier, Jérôme |
| <b>Publisher's version (DOI)</b> | 10.1038/s41550-017-0064  |
| <b>Handle</b>                    | <a href="http://hdl.handle.net/20.500.12386/27146">http://hdl.handle.net/20.500.12386/27146</a>  |
| <b>Journal</b>                   | NATURE ASTRONOMY   |
| <b>Volume</b>                    | 1  |

In the format provided by the authors and unedited.

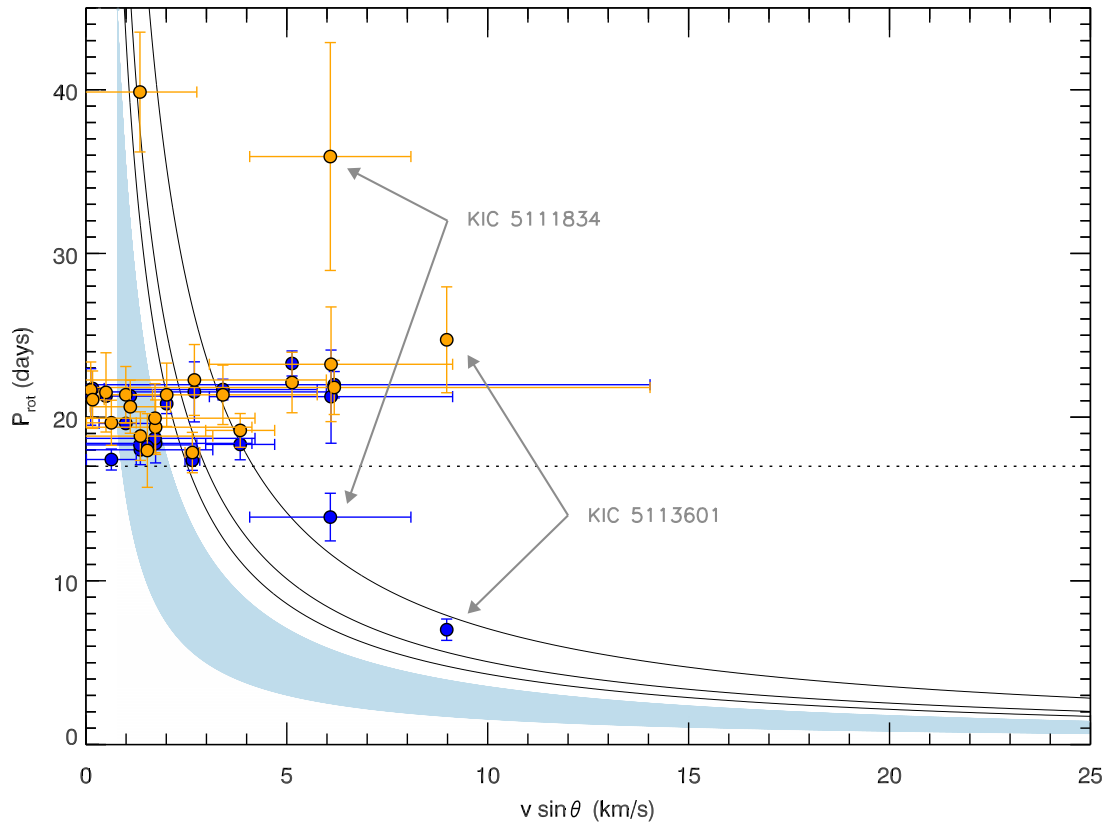
# Spin alignment of stars in old open clusters



**Supplementary Figure 1 | Bayesian peak bagging analysis and fit to the inclination angle.** **a**, A chunk of power spectrum for the core-He-burning red giant KIC 5112373 having a low inclination angle. The Bayesian fit to the oscillations<sup>18,19</sup> is indicated by the red line, with the individual mode frequencies marked by a vertical dotted line and the mode identification by labels. The green and orange vertical bands highlight the regions containing the quadrupole ( $l = 2$ ) and radial ( $l = 0$ ) modes, respectively. The blue bands indicate the three dipolar mixed modes used to fit the inclination angle of the stellar spin (see Methods). The dashed blue line shows the level of the background signal. **b**, A close-up in the region containing the three dipolar mixed modes marked by a blue vertical band, with the red line here showing the resulting Bayesian fit to the inclination angle.



**Supplementary Figure 2 | Comparison of new rotation periods with published values for 30 stars in NGC 6819.** The published rotational periods<sup>20</sup> are compared with the results from our new reanalysis of the same targets (see Methods for more details). Colored symbols correspond to stars discussed in the text (blue circles for clear detection, red squares for unreliable detection, orange triangles for polluted). KIC 4938993, one of the polluted targets, is not displayed because no period measurement could be obtained for this star. The dashed line corresponds to a one-to-one match while the dotted line delimits the threshold of the fast rotating stars selected in this work,  $P_{\text{rot}} = 17$  days. All symbols shown in gray correspond to stars with  $P_{\text{rot}} > 17$  days (circles for clear detections and a square for KIC 5024856, the only slow rotating star with unreliable detection).



**Supplementary Figure 3 | Rotation periods versus published projected equatorial velocities for 21 stars in NGC 6819.** The published rotational periods<sup>20</sup> (blue circles) are compared to those from our analysis (orange circles) for the stars found to have reliable period detections (see Methods). The published  $v \sin \theta$  measurements<sup>20</sup> are kept the same for both sets of period measurements. The horizontal dotted line delimits the threshold of the fast rotating stars discussed here,  $P_{\text{rot}} = 17$  days. The only two fast rotating stars with reliable period detection from our analysis are indicated by arrows, with KIC IDs overlaid. Tracks at constant radii ( $R = 0.85, 1.0, 1.4 R_{\odot}$ ) and inclination angle  $\theta = 90^{\circ}$  are shown. The shaded region delimits a regime of low spin inclination ( $\theta = 20\text{-}30^{\circ}$ ) and stellar radius  $0.85 R_{\odot} \leq R \leq 1.4 R_{\odot}$ .

| KIC ID  | Right Ascension (deg) | Declination (deg) | $\theta$ (deg)  | $\overline{\delta\nu}_{\text{rot}}$ ( $\mu\text{Hz}$ ) | Evolutionary stage |
|---------|-----------------------|-------------------|-----------------|--|--------------------|
| 2297384 | 290.1899              | 37.6641           | $36^{+3}_{-3}$  | 0.055  | RC                 |
| 2297825 | 290.2701              | 37.6843           | $48^{+4}_{-4}$  | 0.050  | RC                 |
| 2436417 | 290.1452              | 37.7750           | $37^{+3}_{-3}$  | 0.063  | RC                 |
| 2436676 | 290.1697              | 37.7912           | $18^{+6}_{-6}$  | 0.250  | RGB                |
| 2436732 | 290.1749              | 37.7984           | $37^{+3}_{-3}$  | 0.072  | RC                 |
| 2436818 | 290.1818              | 37.7349           | $13^{+6}_{-5}$  | 0.180  | RGB                |
| 2437103 | 290.2031              | 37.7868           | $39^{+4}_{-4}$  | 0.121  | RC                 |
| 2437270 | 290.2143              | 37.7780           | $26^{+5}_{-4}$  | 0.122  | RGB                |
| 2437325 | 290.2185              | 37.7876           | $11^{+5}_{-5}$  | 0.150  | RGB                |
| 2437353 | 290.2203              | 37.7592           | $47^{+3}_{-3}$  | 0.066  | RC                 |
| 2437564 | 290.2346              | 37.7426           | $30^{+3}_{-3}$  | 0.070  | RC                 |
| 2437804 | 290.2536              | 37.7594           | $8^{+5}_{-5}$   | 0.050  | RC                 |
| 2437933 | 290.2645              | 37.7771           | $20^{+5}_{-5}$  | 0.200  | RGB                |
| 2437957 | 290.2674              | 37.7730           | $38^{+3}_{-3}$  | 0.184  | RGB                |
| 2437972 | 290.2684              | 37.7694           | $8^{+4}_{-4}$   | 0.150  | RGB                |
| 2437976 | 290.2690              | 37.7815           | $0^{+10}_{-10}$ | 0.180  | RGB                |
| 2437987 | 290.2697              | 37.7656           | $38^{+3}_{-3}$  | 0.057  | RC                 |
| 2438038 | 290.2748              | 37.7994           | $36^{+3}_{-3}$  | 0.045  | RGB                |
| 2438051 | 290.2762              | 37.7499           | $30^{+4}_{-4}$  | 0.062  | RC                 |
| 2438333 | 290.3042              | 37.7168           | $14^{+3}_{-3}$  | 0.080  | RGB                |
| 2569055 | 290.1252              | 37.8387           | $20^{+6}_{-5}$  | 0.120  | RC                 |
| 2569945 | 290.2237              | 37.8399           | $31^{+3}_{-3}$  | 0.083  | RC                 |
| 2570094 | 290.2404              | 37.8170           | $28^{+3}_{-3}$  | 0.066  | RGB                |
| 2570244 | 290.2560              | 37.8014           | $20^{+3}_{-3}$  | 0.172  | RGB                |
| 2570384 | 290.2752              | 37.8680           | $29^{+4}_{-4}$  | 0.040  | RGB                |

**Supplementary Table 1 | Positions and stellar-spin inclinations for the red giants of NGC 6791.** All the declinations and right ascensions refer to the astronomical epoch J2000. The inclination angles are the median values, with corresponding 68.3 % credible intervals, obtained from a Bayesian parameter estimation (see Methods). The average rotational splitting,  $\overline{\delta\nu}_{\text{rot}}$ , is a reference value per star. The evolutionary stage distinguishes between core-He-burning (RC) and shell-H-burning red giants (RGB), and it is derived from the available period spacings used for the peak bagging analysis<sup>16,30,31</sup>.

| KIC ID   | Right Ascension (deg) | Declination (deg) | $\theta$ (deg)  | $\overline{\delta\nu}_{\text{rot}}$ ( $\mu\text{Hz}$ ) | Evolutionary stage |
|----------|-----------------------|-------------------|-----------------|--|--------------------|
| 4937056* | 295.3180              | 40.0975           | $68^{+5}_{-5}$  | 0.084  | RC                 |
| 4937770  | 295.4766              | 40.0360           | $28^{+3}_{-3}$  | 0.265  | RC                 |
| 5023953  | 295.2415              | 40.1382           | $29^{+4}_{-4}$  | 0.204  | RC                 |
| 5024327  | 295.3061              | 40.1989           | $33^{+3}_{-3}$  | 0.112  | RC                 |
| 5024404  | 295.3152              | 40.1696           | $80^{+10}_{-4}$ | 0.125  | RC                 |
| 5024414* | 295.3164              | 40.1865           | $26^{+5}_{-4}$  | 0.351  | RC                 |
| 5024476* | 295.3240              | 40.1544           | $20^{+7}_{-6}$  | 0.180  | RC                 |
| 5024582* | 295.3389              | 40.1992           | $29^{+4}_{-4}$  | 0.141  | RC                 |
| 5111718  | 295.1535              | 40.2548           | $64^{+4}_{-4}$  | 0.249  | RGB                |
| 5111949  | 295.2092              | 40.2197           | $0^{+11}_{-11}$ | 0.200  | RC                 |
| 5112072  | 295.2334              | 40.2277           | $77^{+6}_{-7}$  | 0.220  | RGB                |
| 5112361* | 295.2841              | 40.2524           | $0^{+7}_{-7}$   | 0.150  | RGB                |
| 5112373  | 295.2858              | 40.2250           | $20^{+8}_{-6}$  | 0.120  | RC                 |
| 5112387  | 295.2886              | 40.2455           | $17^{+8}_{-7}$  | 0.150  | RC                 |
| 5112401  | 295.2913              | 40.2638           | $16^{+9}_{-8}$  | 0.080  | RC                 |
| 5112467  | 295.3033              | 40.2066           | $28^{+6}_{-4}$  | 0.137  | RC                 |
| 5112491  | 295.3065              | 40.2057           | $17^{+8}_{-8}$  | 0.150  | RC                 |
| 5112730  | 295.3395              | 40.2326           | $14^{+8}_{-8}$  | 0.120  | RC                 |
| 5112938  | 295.3715              | 40.2178           | $16^{+9}_{-8}$  | 0.120  | RC                 |
| 5112950  | 295.3731              | 40.2059           | $15^{+8}_{-7}$  | 0.170  | RC                 |
| 5112974  | 295.3762              | 40.2561           | $16^{+8}_{-6}$  | 0.150  | RC                 |
| 5113441  | 295.4610              | 40.2670           | $10^{+5}_{-9}$  | 0.500  | RGB                |
| 5200152  | 295.3494              | 40.3624           | $26^{+6}_{-5}$  | 0.149  | RC                 |

**Supplementary Table 2 | Positions and stellar-spin inclinations for the red giants of NGC 6819.** All the declinations and right ascensions refer to the astronomical epoch J2000. The inclination angles are the median values, with corresponding 68.3 % credible intervals, obtained from a Bayesian parameter estimation (see Methods). The average rotational splitting,  $\overline{\delta\nu}_{\text{rot}}$ , is a reference value per star. The evolutionary stage distinguishes between core-He-burning (RC) and shell-H-burning red giants (RGB), and it is derived from the available period spacings used for the peak bagging analysis<sup>16,30,31</sup>. The stars marked with an asterisk are the spectroscopic single-lined binaries<sup>29</sup> indicated in Fig. 1 and 2.

| Simulation # | $E_{\text{ther}}/E_{\text{grav}}$ | $E_{\text{tur}}/E_{\text{grav}}$ | $E_{\text{rot}}/E_{\text{grav}}$ | $\alpha$ |
|--------------|-----------------------------------|----------------------------------|----------------------------------|----------|
| 1            | 0.0025                            | 1.51                             | 0                                | 0.40     |
| 2            | 0.0025                            | 1.12                             | 0.15                             | 0.48     |
| 3            | 0.0025                            | 0.46                             | 0.15                             | 0.45     |
| 4            | 0.0025                            | 0.15                             | 0.15                             | 0.59     |

**Supplementary Table 3 | Energy balancing and alignment parameters of the simulations.** The simulated molecular cloud has a mass of  $10^3 M_{\odot}$  and a radius of 0.084 pc. The various forms of energy used for the different simulations are reported in relative values for the portion of molecular cloud forming the proto-cluster (containing about  $140 M_{\odot}$ ). The thermal energy  $E_{\text{ther}}$ , turbulent kinetic energy  $E_{\text{tur}}$ , and rotational kinetic energy  $E_{\text{rot}}$ , counteract the gravitational potential energy  $E_{\text{grav}}$  and provide global support for the collapsing cloud. The alignment coefficient  $\alpha$  is computed according to its definition (see Methods). All the simulations were run until 25 stars with  $M \geq 0.7 M_{\odot}$  are formed.

| $N$ | $\alpha$          | Skewness |
|-----|-------------------|----------|
| 17  | $0.415 \pm 0.071$ | 2.187    |
| 19  | $0.410 \pm 0.068$ | 2.165    |
| 23  | $0.402 \pm 0.062$ | 2.278    |
| 25  | $0.400 \pm 0.060$ | 2.374    |
| 36  | $0.390 \pm 0.047$ | 2.005    |

**Supplementary Table 4 | Alignment coefficients from simulations of uniform stellar-spin inclination.** The most likely alignment coefficient  $\alpha$  and its  $1\sigma$  uncertainty are computed from a skewed Gaussian probability distribution. The distributions are each obtained from 10000 simulations of random stellar-spin orientation in three dimensions. Each distribution corresponds to a different number of stars,  $N$ . The adopted numbers of stars are chosen according to those from the observations.

| KIC ID   | $\theta$ (deg) | $\overline{\delta\nu}_{\text{rot}}$ ( $\mu\text{Hz}$ ) | Evolutionary stage |
|----------|----------------|--|--------------------|
| 3662421  | $83^{+2}_{-2}$ | 0.163  | RC                 |
| 3744043  | $37^{+3}_{-3}$ | 0.182  | RGB                |
| 3954857  | $86^{+4}_{-2}$ | 0.149  | RC                 |
| 3965149  | $42^{+6}_{-6}$ | 0.096  | RC                 |
| 4253026  | $75^{+2}_{-2}$ | 0.108  | RC                 |
| 5709182  | $38^{+3}_{-3}$ | 0.084  | RC                 |
| 6117517  | $18^{+3}_{-3}$ | 0.274  | RGB                |
| 6144777  | $61^{+2}_{-2}$ | 0.177  | RGB                |
| 6363338  | $90^{+4}_{-4}$ | 0.170  | RC                 |
| 6535641  | $24^{+5}_{-5}$ | 0.040  | RC                 |
| 6604616  | $90^{+4}_{-4}$ | 0.093  | RC                 |
| 6936990  | $72^{+3}_{-3}$ | 0.058  | RC                 |
| 7025568  | $42^{+2}_{-2}$ | 0.149  | RC                 |
| 7060732  | $79^{+1}_{-1}$ | 0.225  | RGB                |
| 7619745  | $90^{+8}_{-8}$ | 0.228  | RGB                |
| 8366239  | $74^{+3}_{-3}$ | 0.149  | RGB                |
| 8475025  | $90^{+3}_{-3}$ | 0.229  | RGB                |
| 8547122  | $83^{+5}_{-4}$ | 0.091  | RC                 |
| 8718745  | $23^{+2}_{-2}$ | 0.287  | RGB                |
| 9145955  | $10^{+6}_{-6}$ | 0.180  | RGB                |
| 9267654  | $90^{+3}_{-3}$ | 0.312  | RGB                |
| 9412305  | $58^{+5}_{-5}$ | 0.081  | RC                 |
| 9475697  | $32^{+3}_{-3}$ | 0.222  | RGB                |
| 9779708  | $38^{+3}_{-3}$ | 0.045  | RC                 |
| 9882316  | $0^{+6}_{-6}$  | 0.400  | RGB                |
| 9907009  | $46^{+4}_{-4}$ | 0.058  | RC                 |
| 10014635 | $30^{+3}_{-4}$ | 0.082  | RC                 |
| 10123207 | $0^{+3}_{-3}$  | 0.400  | RGB                |
| 10200377 | $0^{+3}_{-3}$  | 0.300  | RGB                |
| 10257278 | $84^{+4}_{-3}$ | 0.332  | RGB                |
| 11200291 | $28^{+3}_{-3}$ | 0.042  | RC                 |
| 11353313 | $72^{+2}_{-2}$ | 0.346  | RGB                |
| 11570459 | $54^{+3}_{-3}$ | 0.052  | RC                 |
| 11913545 | $90^{+5}_{-5}$ | 0.196  | RGB                |
| 11968334 | $56^{+2}_{-2}$ | 0.283  | RGB                |
| 12008916 | $90^{+5}_{-5}$ | 0.299  | RGB                |

**Supplementary Table 5 | Stellar-spin inclinations for the control sample of field red giants.** The control sample includes the 19 shell-H-burning red giants with detailed peak bagging parameters already available<sup>19</sup>, and additional 17 core-He-burning red giants<sup>36</sup>. All the inclination angles were measured using the same approach as for the cluster stars. The inclination angles are the median values, with corresponding 68.3 % credible intervals, obtained from a Bayesian parameter estimation (see Methods). The evolutionary stage is obtained from published period spacings<sup>19,31,35</sup>. The average rotational splitting,  $\overline{\delta\nu}_{\text{rot}}$ , is a reference value per star.